

# Metal-insulator phase transition and structural stability in 'Sb' doped $\text{CaMnO}_3$ perovskite

R. Kannan<sup>1,\*</sup>, D. Vanidha<sup>1</sup>, A. Arun Kumar<sup>1</sup>, K. U. Rama Tulasi<sup>1</sup>, R. Sivakumar<sup>2</sup>

<sup>1</sup>Department of Physics, Pondicherry Engineering College, Pondicherry-605 014, India

<sup>2</sup>Department of Physics, Pondicherry University, Pondicherry-605 014, India

## Email address:

kannan@pec.edu(R. Kannan)

## To cite this article:

R. Kannan, D. Vanidha, A. Arun Kumar, K. U. Rama Tulasi, R. Sivakumar. Metal-Insulator Phase Transition and Structural Stability in 'Sb' Doped  $\text{CaMnO}_3$  Perovskite. *International Journal of Materials Science and Applications*. Vol. 2, No. 4, 2013, pp. 128-135.

doi: 10.11648/j.ijmsa.20130204.12

---

**Abstract:** Electron doped  $\text{Ca}_{1-x}\text{Sb}_x\text{MnO}_3$  ( $X = 0$  to  $0.4$ ) compound when prepared by high temperature solid state reaction, exhibits orthorhombic distorted perovskite structure. A systematic, continuous doping increases the metal – insulator transition temperature to above the room temperature ( $\approx 431$  to  $469$  K); due to the mismatch of ionic radii in A site rising anti - site effect, which consequently changes the bond length. Doping induced metal – insulator transition accompanied by structural transition is reflected through the drastic changes in the parameters like cation size variance factor ( $\sigma$ ), average ionic radius  $\langle r \rangle$ , tolerance factor ( $t$ ) and  $T_0$ -which is correlated to the band related transport properties. Structural transition from the phase of perovskite to Brownmillerite has been found for the compositions  $x = 0.3$  and  $0.4$ , which is attributed due to the ionic radii mismatch. Doping exerts chemical pressure by modifying compression of A-O bond and relaxation of B-O bond, giving rise to strain similar to external pressure in  $\text{ABO}_3$  perovskite. The dependence of electrical transport at high temperature has been studied, by employing variable range hopping and small polaron hopping model as an account for the experimental observation due to disorder induced localization.

**Keywords:** Phase Transition, Pervoskite, High  $T_c$

---

## 1. Introduction

In manganites, optimum grain size for preferential orientations the need of the hour for low field magnetoresistance (LFMR) applications at ambience in the applied magnetic field for 100% spin polarization between the grains. Storage and retrieval of information from computer hard disk were revolutionized after the discovery of colossal magneto resistance (CMR) based manganite read/write heads. Miniaturization, Storage increase and High magneto resistance (MR) through LFMR, kept further renewing the interest in CMR even after three decades of fundamental researches on manganite [1, 2]. However, the origin of conductivity in doping induced disordered oxide materials is not yet clear due to charge localization. The parameters like dopant atom, particle size and pressure are varied in perovskite manganites to achieve metal – insulator transition temperature ( $T_{MI}$ ) above the room temperature.

$\text{CaMnO}_3$  is an antiferromagnetic Mott-Hubbard insulator known for becoming metallic in nature at narrow doping

levels itself, as  $\text{CaMnO}_3$  is at the edge of Metal-Insulator (M-I) transition. For electron doped CMR compounds, due to the high efficiency and minimum disorder  $\text{AMnO}_3$  ( $A=\text{Ba}, \text{Ca}, \text{Sr}$ ) is most preferred when compared to  $\text{LaMnO}_3$ . In those compounds anti-ferromagnetic (AFM) to paramagnetic (PM) transition was reported by Esa Bose et al [3]. Doping induced structural changes are reported by Qingdi Zhou et al [4] in  $\text{SrMnO}_3$ , since MR is intrinsically connected to metal - insulator transition and charge orbital ordering. Electron doping induced cubic to tetragonal and cubic to orthorhombic phases was reported by Brendan J. Kennedy et al [5] in tetravalent Cerium ( $\text{Ce}^{4+}$ ) doped  $\text{SrMnO}_3$  due to Jahn Teller co-operative tilting of  $\text{MnO}_6$  octahedra. High temperature resistivity of Sb doped  $\text{CaMnO}_3$  [6] exhibits decrease in conductivity with increase in temperature and  $d\sigma/dT$  became negative at around  $600^\circ\text{C}$  indicating a transition from semiconducting to metallic.

$\text{CaMnO}_3$  when doped with  $\text{Sb}^{5+}$  ion produces excess electrons through  $\text{Mn}^{4+}$  to  $\text{Mn}^{3+}$  conversion. Ping Duan et al [7] proved the existence of mixed valence states of Mn ( $\text{Mn}^{3+}$  and  $\text{Mn}^{2+}$ ) through XPS (X-ray photoemission

spectroscopy) and upon Sb doping Curie temperature ( $T_c$ ) reaches a value of 245 K in  $\text{La}_{1-x}\text{Sb}_x\text{MnO}_3$  for  $x = 0.1$ . High phase transition temperature ( $\approx T_p \Rightarrow$  temperature at which maximum resistivity occurs) of 289 K has been recorded for La doped  $\text{Mn}^{2+}$  rich compound  $\text{BaMnO}_3$  for  $x=0.3$  [1].

$\text{Sb}_2\text{O}_3$  during the synthesis acts not only as reactant but also as an additive for decreasing the reaction temperature for phase formation from  $1200^\circ\text{C}$  to  $900^\circ\text{C}$ . The decreased reaction temperature for phase formation is due to the change in the eutectic point [8] of the mixture of all the reactants since additives provide liquid – phase grain growth at low temperature [9, 10]. Thus the synthesis at a temperature less than the eutectic temperature of a mixture enhances the phase formation and control of particle size [11]. High reaction temperature for phase formation, non-homogeneous mixing and agglomeration are commonly found in synthesis of oxide materials by solid state reaction [12]. Hence, the decreased reaction temperature is one of the reasons for increased Metal – Insulator transition temperature to 431 K compared to literature value 420 K [13].

In the present work we are discussing the electrical transport properties of the ‘Sb’ doped  $\text{Ca}_{1-x}\text{Sb}_x\text{MnO}_3$  ( $x=0$  to 0.4), fabricated by low temperature sintering method. Doping induced structural phase transition accompanied by metal - insulator phase change has lead to a record high temperature of 431 K, as the  $T_{MI}$  for  $x=0.2$  in ‘Sb’ doped  $\text{CaMnO}_3$  is a consequence of A site doping. This is attributed to very large difference in ionic radii, ‘Sb’ (0.74 Å) atom occupies Mn (0.53 Å) site instead of Ca (1.12 Å) site making A/B cation ratio deviating from perovskite structure. Doping induced charge localization and along with phase transition leading to changes in the density of states and resistivity are found from the  $T_o$  values [14].

## 2. Experiment

The electron doped bulk samples of  $\text{Ca}_{1-x}\text{Sb}_x\text{MnO}_3$  were prepared by high temperature solid-state reaction method. Highly pure  $\text{CaCO}_3$  (Merck, 99.9%),  $\text{Sb}_2\text{O}_3$  (Merck, 99.9%) and  $\text{MnO}_2$  (Merck, 99.9%) were taken in the stoichiometry ratio and thoroughly mixed and ground until uniform mixing and homogeneous distribution is achieved. The finely grounded samples were taken in an alumina crucible and calcined in air at  $900^\circ\text{C}$  for 12 hours. The resulting powders were pelletized using hydraulic press in to small disks of 8 mm diameter and 1 mm to 2mm thickness under a pressure of 3 to 5 tons. All those pellets prepared were sintered at  $900^\circ\text{C}$  continuously or 36 hours and cooled to room temperature.

All the five samples of  $\text{Ca}_{1-x}\text{Sb}_x\text{MnO}_3$  ( $x=0$  to  $x=0.4$ ) were prepared under exact heating conditions as described above. The samples are characterized by powder XRD (Rich-Seifert, Germany) using  $\text{Cu K}\alpha$  radiation. Electrical transport studies were carried out using Silver electrodes of 99.9% purity with Keithley electrometer (Model 617).

## 3. Results and Discussion

### 3.1. XRD Analysis

XRD pattern of polycrystalline  $\text{Ca}_{1-x}\text{Sb}_x\text{MnO}_3$  ( $X = 0$  to 0.4) samples belonging to orthorhombic structure are shown in fig 1(a). In ‘Sb’ substituted samples, splitting of the X-ray peak (112) into (002) and (112) for  $x = 0.1, 0.2, 0.3$  and  $x = 0.4$  was observed and attributed to the increased orthorhombicity of the compound. Average grain size is estimated using Scherrer’s formula  $D = k\lambda/\beta\cos\theta$  [14] and it is found to be increasing as a function of increasing composition of ‘x’ which are tabulated in table 1. Crystallite size changes consistently with doping as 12 nm for  $x=0.1$ , 21 nm for  $x=0.2$ , 27 nm for  $x=0.3$ . Extreme end members  $x=0$ , i.e. undoped compound crystallizes at 15nm and for  $x=0.4$ , it is found to be 66 nm, due to phase segregation and limited solubility. Smaller particle size of 12-27 nm comparable to wet chemical methods are attributed due to long time sintering for 36 hours at low temperature (i.e)  $900^\circ\text{C}$ . The smaller particle size due to low sintering temperature are attributed to the assistance of  $\text{Sb}_2\text{O}_3$  as sintering aid like  $\text{Bi}_2\text{O}_3$  and  $\text{Li}_2\text{CO}_3$  in synthesis of dielectrics [9,15].

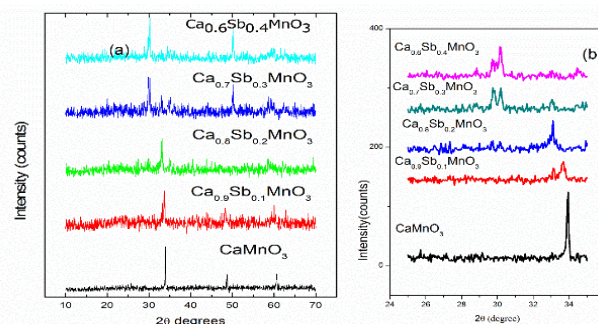


**Fig 1.** (a) XRD pattern of  $\text{Ca}_{1-x}\text{Sb}_x\text{MnO}_3$  ( $0 \leq x \leq 0.4$ ) (b) Shifting of 112 peak of  $\text{Ca}_{1-x}\text{Sb}_x\text{MnO}_3$  ( $0 \leq x \leq 0.4$ )

Lattice parameters of orthorhombic crystal structure as a function of Sb doping was found to be increasing from 4.8403 Å to 5.3213 Å for ‘a’, indicating that  $\text{Ca}^{2+}$  being replaced by  $\text{Sb}^{5+}$  along ‘a’ axis. This produces a corresponding compression in ‘b’ axis from 5.8426 Å to 5.3834 Å making the tolerance factor ‘t’ stable [Table 2]. The ‘c’ axis also found to undergo an elongation from 7.5401 Å to 7.7405 Å for doping concentration of  $0.3 \leq x \leq 0.4$ . Increase in the lattice parameter for the concentration  $x = 0.2$  to 0.4, indicates low chemical pressure induced by doping giving rise to high transition temperature [16].

Doping induced structural disorder was found from the XRD for concentrations  $x = 0.3$  and  $x = 0.4$ . Due to large difference in ionic radii, Sb (0.74 Å) atom occupies Mn (0.53 Å) site instead of Ca (1.12 Å) site making A/B cation ratio deviating from one. Brownmillerite phase [17] of stoichiometry composition  $(\text{Ca}_{1-x}\text{Sb}_x)[\text{Mn}]\text{O}_3$  becomes  $(\text{Ca}_{1-x})[\text{Sb}_x\text{Mn}]\text{O}_3$ , which was ascertained from the disappearance of characteristic perovskite 112 peak at  $2\theta =$

$34^\circ$  and appearance of (002) peak at  $2\theta = 31.5^\circ$  degrees of Brownmillerite phase as shown in fig1(b). This gives rise to a non-uniform change in the lattice parameters due to chemical doping pressure and cell volume  $213.2 \text{ (\AA)}^3$  to  $249.9 \text{ (\AA)}^3$ . The structural distortion produced by both the phases having orthorhombic in common is a measure of average A-size cationic radius  $\langle r_A \rangle$  and size variance factor ( $\sigma^2$ ).

### 3.2. Electrical Transport Properties

Resistivity ( $\rho$ ) as a function of temperature ( $T$ ) from 303 to 673 K is shown in the Fig.2. All the  $\rho$  - $T$  curves exhibit the same behavior indicating similar structure and phase

formation undergoing M-I phase transition at 303 K, 431 K, 435 K and 468 K for  $x = 0.1$  to 0.4 respectively. For  $x = 0$ , which corresponds undoped compound do not show  $T_{MI}$  since it is AFM insulator. The increased  $T_{MI}$  for concentrations  $x = 0.3$  and 0.4 is attributed to anti-site doping disorder, at which perovskite phase become Brownmillerite phase [17]. Low sintering temperature, presence of excess  $\text{Mn}^{4+}$  due to Sb doping (increase in  $\text{Mn}^{3+} / \text{Mn}^{4+}$ ) ratio, nature of ‘Sb’ as both reactant and additive and structural changes due to lattice mismatch between ‘Sb’ and ‘Ca’ ionic radii are all cannot be denied as possible causes for increased  $T_{MI}$ .

**Table 1:** Lattice Parameter, Unit Cell Volume, Metal insulator Transition Temperature ( $T_{MI}$ ), And Crystalline Size of  $\text{Ca}_{1-x}\text{Sb}_x\text{MnO}_3$  ( $0 \leq x \leq 0.4$ ).

Crystalline size (nm)	15	12	21	27	66
pat Tp	-	9.34	171.17	172.23	61.042
K $\Omega$ cm					
pat 303K	16.910	8.542	0.1219	22.298	0.355
K $\Omega$ cm					
TMI (K)	-	303	431	435	468
V ( $\text{\AA}$ )	219.9	213.2	223.7	221.8	249.9
c ( $\text{\AA}$ )	7.306	7.540	7.658	7.740	7.5146
b ( $\text{\AA}$ )	5.789	5.589	5.507	5.383	6.000
a ( $\text{\AA}$ )	5.200	4.840	5.303	5.323	5.424
System	CaMnO3	Ca0.9Sb0.1MnO3	Ca0.8Sb0.2MnO3	Ca0.7Sb0.3MnO3	Ca0.6Sb0.4MnO3

**Table2:** Ionic Radius, Size Variance Factor, Tolerance Factor,  $T_0$ , Activation Energy of  $\text{Ca}_{1-x}\text{Sb}_x\text{MnO}_3$  ( $0 \leq x \leq 0.4$ ).

System	Ionic radius $\langle r_A \rangle$ ( $\text{\AA}$ )	Size variance factor $\sigma^2$ ( $\text{\AA}$ )	Tolerance factor ‘t’	T0 from VRH model X108	Small polaron hopping Activation Energy in (eV)
CaMnO3	-	-	-	8.78	0.3875
Ca0.9Sb0.1MnO3	1.136	0.0175	0.9315	2.44	0.5596
Ca0.8Sb0.2MnO3	1.092	0.0310	0.9152	1.722	1.0441
Ca0.7Sb0.3MnO3	1.048	0.0405	0.8989	1.694	0.8582
Ca0.6Sb0.4MnO3	1.004	0.0464	0.8826	2.3868	1.0786

The room temperature resistivity of the samples decreases from 16.95  $\text{K}\Omega\text{cm}$  ( $x = 0.0$ ) to 0.1219  $\text{K}\Omega\text{cm}$  ( $x=0.2$ ) upon systematic doping, is attributed to the increase in the charge carrier concentration ( $\text{Sb}^{5+}$  introduces twice as many electrons per  $\text{Ca}^{2+}$  atom) enabling double exchange (DE) mechanism [7]. Every  $\text{Sb}^{5+}$  dopant atom makes two  $\text{Mn}^{4+}$  ions converted into two  $\text{Mn}^{3+}$  ions and electron hopping between ‘Mn’ ions is responsible for electrical conductivity in perovskite manganites, and it also indicates that the dopant atom ‘Sb’ exactly replaces ‘Ca’ making the double exchange possible up to  $x= 0.2$ . For increased concentrations, resistivity increases to 23.205  $\text{K}\Omega\text{cm}$  and then decreases to 0.355  $\text{K}\Omega\text{cm}$  respectively for  $x=0.3$  and  $x$

$= 0.4$  as shown in table 1. The abrupt rise in resistance for  $x=0.3$  is assigned to Jahn-Teller distortion indicating that no more double exchange is possible, favoring the insulating state due to localization of electrons [18,19]. The decreased resistivity of three order for  $x=0.4$ , is due to increased grain size of almost three times (27 nm to 66 nm respectively for  $x=0.3$  to  $x = 0.4$ ) and also due to the appearance of Brownmillerite phase different from the perovskite phase. The peak resistivity is also found to follow the similar trend with the exception for  $x=0.2$ . The abrupt change in size variance factor ( $\sigma^2$ ) from 0.0175 to 0.0310 respectively for  $x=0.1$  and  $x = 0.2$  is responsible for the observed change that are tabulated in table 2.

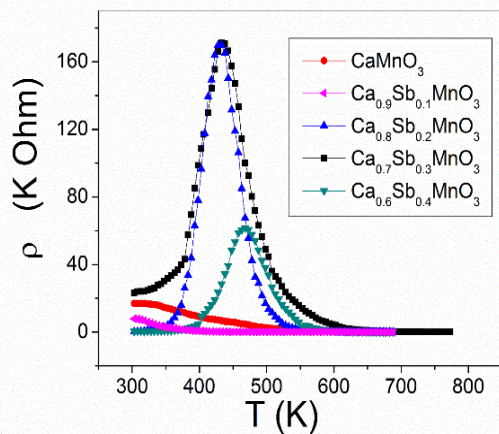


Fig 2. Resistivity versus temperature of  $Ca_{1-x}Sb_xMnO_3$  ( $0 \leq x \leq 0.4$ )

The origin of Brownmillerite phase is attributed to limited solubility which leads to anti-site effect. Increased dopant concentration produces a chemical pressure, giving rise to a compression in the A-O bond and relaxation in B-O bond making similar to external pressure which modifies the local structure of distorted orthorhombic perovskite (Pbma) to distorted orthorhombic Brownmillerite structure (Pbam) [17,20]. Abrupt reduction in the peak height and broadening in the ( $\rho$ -T) curve for the composition  $x=0.3$  and  $x=0.4$  is also another form of evidence for the chemical pressure induced formation of Brownmillerite phase. Hence, the limit of increase of  $T_{MI}$  with doping is subjected to structural stability and beyond which it cannot be increased.

From the above experimental observations, we may conclude that the low sintering temperature and flux wrapping of  $Sb_2O_3$  disfavors the formation of large grains [21,22]. Therefore, the average grain size decreases (12 nm to 27 nm for  $x=0$  to  $x=0.3$  and 66 nm for  $x=0.4$ ) compared to normal and the grain boundary effect increases. This prevents the charge carriers from crossing the boundary between the neighboring grains leading to charge localization. Because of the increased grain boundary effect the resistivity is largely increased over the whole range of temperature studied [14]. This may be inferred from the peak broadening in XRD and consequently due to smaller particle size, grain boundary volume ratio is greater than the grains giving rise to high resistance.

High value of resistance ( $M\Omega$ ) in Semiconducting-Insulating region is attributed to lattice mismatch (Ca/Sb) and appearance of Brownmillerite phase due to anti-site doping induced structural distortion; which in turn related to distortion favours insulating state due to localization of electrons as discussed earlier [18,19]. Klien et al [21] reported that the lattice strain is mainly responsible for the anomalies like phase segregation and magnetic interphase disorder, which gives rise to high resistance at room temperature. Resistance dependence of temperature gives information of disordering across the grain boundaries.

### 3.3. Modeling

The experimentally observed  $\rho$ -T curves of  $Ca_{1-x}Sb_xMnO_3$  samples are considered as the superimposition of two different transport phenomena named AFM metal-like behavior below  $T_c$  and PM insulating behavior above  $T_c$ . The metal like nature below  $T_c$  is explained with Zener's DE mechanism with a resistivity equation of the type  $\rho(T) = \rho_0 + \rho_2 T^2 + \rho_n T^n$  [23] and pure magnon scattering is represented by the equation  $\rho(T) = \rho_0 + \rho_2 T^\alpha$  [24,25] are fitted separately here. The corresponding  $\rho_0$  values are  $0.185 \times 10^6$  ( $0.1168 \times 10^6$ )  $\Omega cm$  for  $Ca_{0.8}Sb_{0.2}MnO_3$ ,  $0.270 \times 10^6$  ( $0.166 \times 10^6$ )  $\Omega cm$  for  $Ca_{0.7}Sb_{0.3}MnO_3$  and  $0.069 \times 10^6$  ( $0.044 \times 10^6$ )  $\Omega cm$  for  $Ca_{0.6}Sb_{0.4}MnO_3$  for both the models found to be high due to disorder induced localization.

At above  $T_c$  in all the  $\rho$ -T curves, it is observed a deviation from the linearity when the temperature is close to 550 K, where the rising of peak resistivity starts. This deviation indicates a crossover from activated carrier to another transport mechanism. The sudden drop in resistivity over a very narrow temperature range of 431 K to 523 K and saturation over wide range of temperature 550 K to 773 K, constitutes a clear evidence of change in the transport mechanism. Hence, the semiconducting - insulating part of the  $\rho$  (T) curve was found to exhibit two different regimes. This abrupt change in resistivity when it is close to the peak is explained by two different models in an account of the actual experimental observations. It explains, to understand the transport mechanism in doping induced disordered oxide CMR materials at high temperature regime [14,26,27] as a variable range hopping  $\rho = \rho_0 \exp(-T_0/T)$  and a small polaron hopping  $\rho = B T \exp(E_p/k_B T)$ .

### 3.4. Variable Range Hopping Mechanism (VRH)

Conducting behaviour in manganites is explained based on doping induced disorder which gives rise to localization of energy states close to fermi level between conduction band and valence band. At high temperatures, carriers are thermally activated to their nearest neighbour site with high mobility. But when temperature decreases, thermally activated behaviour decreases and hopping process dominates, and conduction takes place by hopping of charge carriers between the localized states distributed unevenly. Normally carrier localization at the grain boundary changes the conductivity to semiconducting or insulating and carrier delocalization leads to metal like behaviour. The hopping is characterized by the parameter  $T_0$  which is related to electronic density of states  $N(E_F)$  and radius of localization length ( $a$ ) by  $T_0 = 18/k_B N(E_F) a^3$ . High  $T_0$  value indicates multiphonon hopping with a large increase in the localization length and increase in barrier height at the grain boundaries leads to insulating and if  $T_0$  decreases, based on hopping range and energy, the material remains in the metallic state of mott's transition [8,19]. Size of the grain and width of grain boundary in the order of



nanometers (or the localization length 'a' ( $1/\alpha$ )) will correspond to 100% spin polarization by tunneling mechanism [28,29].

The resistivity data in insulator regime were fitted to the variable range hopping (VRH) proposed by Mott as shown in Fig.3 linearizing the equation  $\rho = \rho_0 \exp(T_0/T)^{1/4}$  and from the slope  $T_0$  values are obtained. In the present work, for every one 'Sb<sup>5+</sup>' doped in CaMnO<sub>3</sub>, makes two Mn<sup>4+</sup> ions which is transferred to two Mn<sup>3+</sup> ions due to rich in electron carrier makes the carrier density  $N(E_F)$  of the system fixed. Since VRH takes place due to excitation of charge carrier across coulomb gap ( $W/U \gg 1$ ), Ponnambalam et al [30] reported VRH mechanism over a very large temperature range of 100 K to 900 K.

Variation of  $T_0$  with doping concentration ( $8.78 \times 10^8$  to  $1.694 \times 10^8$ ), decreases uniformly for  $x = 0$  to  $x = 0.3$  indicating the reduction in the disorder, which in turn changes the Mn-O-Mn bond and leads to increase in the carrier concentration which is attributed to altering of ( $t_{2g}$ - $e_g$ ) orbitals by giving rise to drastic change in the band width due to electron filling [31,32] except for  $x = 0.4$ . And

for  $x = 0.4$ ,  $T_0$  further increases to  $2.3868 \times 10^8$  indicating Jahn-Teller distortion along with structural phase transition to Brownmillerite phase for  $x > 0.3$ . The decrease of  $T_0$  due to low sintering temperature indicates the improvement in the crystallinity and hence the quantum mechanical tunnelling between the disorder induced localized state increases reducing the resistivity.

This variations in  $T_0$  is attributed to the variations of ( $\sigma^2$ ) compared to CaMnO<sub>3</sub> and SrMnO<sub>3</sub> as shown in the Table 3. The increase in  $T_0$  value observed for our system is correlated to the structural variations caused due to the doping induced cation size disorder ( $\sigma^2$ ) [33,34].

The overall fitting of our experimental data observation indicates that at temperatures where the thermal energy is very low, the VRH model perfectly fits perfectly to the equation and at the temperature where the thermally activated process dominates the experimental data deviates from the fitted data as shown in the Fig.3. Moreover, the fitted model of VRH proves localizations of charge carriers created by doping induced disorder are mainly responsible for the electrical conduction process in manganites.

**Table 3:**  $T_0$ , Cation Size Variance Factor, Activation Energies of some reported systems along with present work.

System	$T_0$	Activation energy	Cation size variance $\sigma^2 = \sum y_i^2 - \langle y \rangle^2$	Reference
Ca <sub>1-x</sub> Sb <sub>x</sub> MnO <sub>3</sub> (Sb=0, 0.1, 0.2, 0.3, 0.4)	$2.333 \times 10^8$ to $1.88 \times 10^9$	0.3875 to 1.0786 (eV)	0.0175 to 0.0464	Present Work
LaMnO <sub>3</sub>	$1.23 \times 10^2$ to $1.601 \times 10^6$	163 to 248.9 (meV) (VRH)		Ref 29
La(NiFe)O <sub>3</sub>	$1.87 \times 10^2$ to $1.7 \times 10^7$	10 to 206 (meV) (VRH)		Ref 32.
(NdLnSr)MnO <sub>3</sub>	$0.42431 \times 10^6$ to $18.4 \times 10^6$	61.48 to 160.03 (meV) (SPH)		Ref 35.
LaCaMnO <sub>3</sub>		92 to 116 (meV) (SPH)		Ref 36.
LaSrMnO <sub>3</sub>	$4.3 \times 10^7$ to $1.3 \times 10^8$			Ref 21.
Ca <sub>1-x</sub> R <sub>x</sub> MnO <sub>3</sub> (R=La, Pr, Nd, Sm, Eu, Gd, Tb, Dy, Ho, Er, Yb) ( $x=0.1$ )		56.9 (meV) to 65.6 (meV) (SPH)	$1.54 \times 10^{-3}$ to $3.6 \times 10^{-7}$	Ref 40.
Sr <sub>1-x</sub> AxMnO <sub>3</sub> ( $x=0$ to 1) (A=Ca)			$2.5 \times 10^{-3}$ to $9 \times 10^{-4}$	Ref 33.

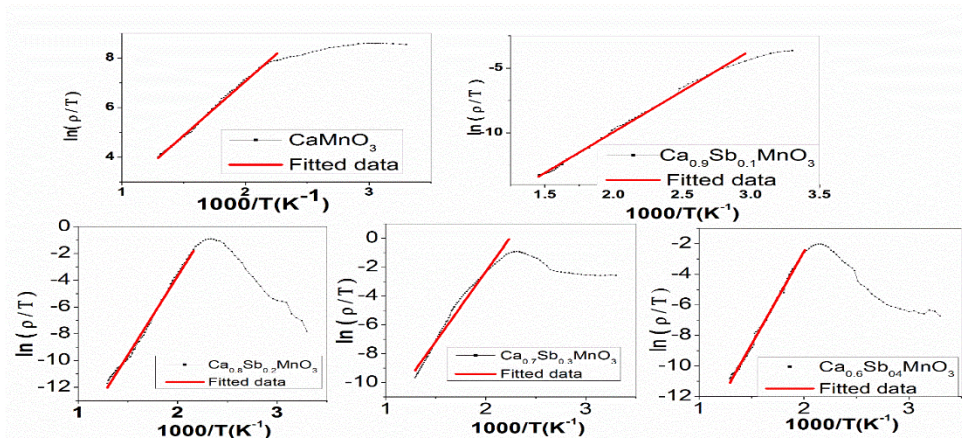


**Fig. 3.** Variable range hopping of Ca<sub>1-x</sub>Sb<sub>x</sub>MnO<sub>3</sub> ( $0 \leq x \leq 0.4$ ) [ $\ln(\rho/T)$ ] vs  $1/T^{1/4}$

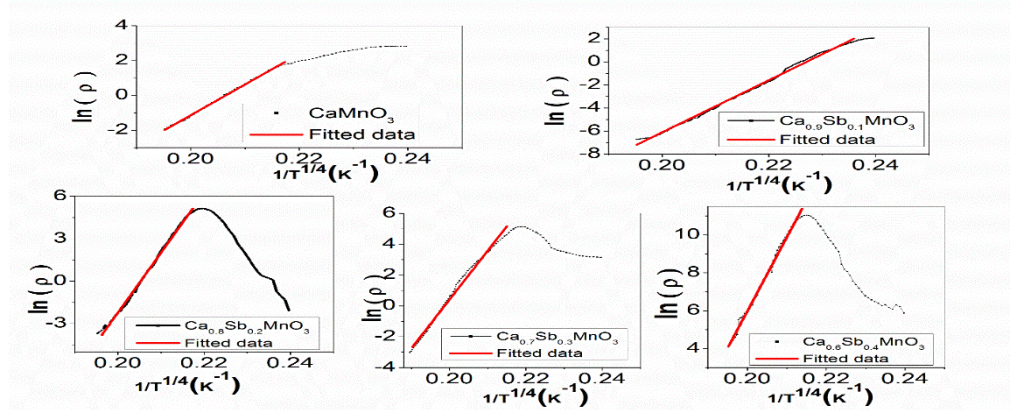


Fig. 4. Adiabatic small polaron hopping of  $\text{Ca}_{1-x}\text{Sb}_x\text{MnO}_3$  ( $0 \leq x \leq 0.4$ ) [ $\ln(\rho/T)$  vs  $1000/T$ ]

### 3.5. Small Polaron Hopping Model

Zener's double-exchange model will not be sufficient enough to explain the very large change in resistivity in the Semiconducting-Insulating phase i.e., at high temperature region, since it does not consider spin-lattice or charge-lattice interactions, i.e., Jahn-Teller (JT) interaction and polarons, which significantly contribute [14] to the conduction process in the Semiconducting-Insulating phase. Therefore, it is very essential to understand the electrical conduction in the Semiconducting-Insulating region (where  $T \gg T_{\text{MI}}$ ) which is governed by polaronic effects [20,21]. The conduction mechanism in manganites at high temperatures is governed by thermally activated small polarons based on the polaronic models.

The resistivity data in Semiconducting-Insulating region were fitted to the adiabatic small polaron hopping (ASPH) equation  $\rho = B T \exp(E_p/k_B T)$  where  $B = [k_B/v_{\text{ph}} N e^2 R^2 C (1-C)] \exp(2\alpha R)$ ,  $k_B$  is the Boltzmann constant, and  $T$  is the absolute temperature,  $N$  is the number of ion sites per unit volume,  $R$  is the average intersite spacing obtained from the relation  $R = (1/N)^{1/3}$ ,  $C$  is the fraction of sites occupied by the polaron,  $\alpha$  is the electron wave function decay constant,  $v_{\text{ph}}$  is the optical phonon frequency ( $v_{\text{ph}} = k_B \theta_D / h$ ) and  $E_p$  is the activation energy following Padmavathi et al [35], Sayani Bhattacharyar [36], Abdel-Khalek et al [37] and Wasi Khan et al [29] for our system as shown in Fig.4. The temperature dependent polaron hopping is verified by calculating  $\theta_D/2$  ( $\theta_D =$  Debye's temperature), where deviation from linearity occurs in the  $\ln(\rho/T)$  vs  $1/T$  plot and the estimated phonon frequency. Leaving the undoped compound for concentrations  $x = 0.1$  to  $0.4$ ,  $\theta_D/2$  and  $v_{\text{ph}}$  (optical phonon frequency) are found to be varying linearly from 356 K, 459 K, 480 K, 495 K and  $7.44 \times 10^{12}$ ,  $9.53 \times 10^{12}$ ,  $9.9 \times 10^{12}$ ,  $10.35 \times 10^{12}$  respectively and in agreement with the reported values [30, 33].

The activation energy  $E_p$  was found to be increasing continuously with the doping concentration from 0.5596 to 1.044 eV for  $x = 0.1$  to  $0.2$  indicating the presence of perovskite phase and it varies from 0.8582 to 1.0786 eV for  $x = 0.3$  and  $x = 0.4$ , which is attributed to the appearance of brownmillerite phase and increase in the localization of

charge carriers [38]. The increase in the activation energy is attributed to structural phase transition associated with the inhomogeneity or disorder in the barrier height and width. As well, the insufficient crystallization of 'Sb' in the system due to low sintering temperature ( $900^\circ\text{C}$ ) also cannot be ruled out.

Very large variations in ( $\sigma^2$ ) compared to  $\text{CaMnO}_3$  and  $\text{SrMnO}_3$  as listed in the Table 3 is attributed to the large difference in the ionic radii between Ca ( $\text{Ca} = 1.12 \text{ \AA}$ ) and Sb atom ( $\text{Sb} = 0.74 \text{ \AA}$ ) which is due to anti-site doping induced cation disorder [28,39] and appearance of brownmillerite phase at higher 'Sb' concentrations. This gives rise to large value of activation energy compared to other system as listed in Table 3. Hence, this results indicate structural parameter  $\sigma^2$  is closely related to electrical transport properties. Existence of higher activation energy is attributed to crystal distortions which increases the potential barrier height for polaron hopping [40]. When  $\sigma^2$  varies from 0.0175 to 0.0464 activation energy is found to be 387.5 to 1078.6 (meV) (SPH) where as Yang Wang et al [40] reported the activation energy in the range of 56.9 to 65.6 (meV) for the  $\sigma^2$  in the range of  $1.54 \times 10^{-3}$  to  $3.6 \times 10^{-7}$ . In fact, this may be compared with Ca/Sb ratio to Ca/RE ionic radii ratio.

## 4. Conclusion

We have investigated the effect of 'Sb' doping on the structural and electric transport properties of  $\text{CaMnO}_3$  in orthorhombic structure. The doping of 'Sb' for the first time increases  $T_{\text{MI}}$  to a maximum of 468 K for  $x = 0.3$ . The shifting of  $T_{\text{MI}}$  towards high temperature is attributed to the presence of Brownmillerite phase due to limited solubility of 'Sb' at 'Ca' site and increase in the lattice parameter for the concentration  $x = 0.2$  to  $x = 0.4$ , which indicates low chemical pressure induced by doping. Increased concentration of 'Sb' produces doping induced structural distortion from perovskite phase to Brownmillerite phase which is confirmed from the disappearance of characteristic perovskite at high intense 112 peak, which is very well reflected in the tolerance factor ( $t$ ), average ionic radii  $\langle r_A \rangle$  and size variance factor  $\sigma^2$ . Low sintering temperature

favors large change in resistance ratio, increased  $T_{MI}$ , liquid-phase grain growth and flux wrapping of 'Sb' yields smaller sized crystallites. Also, increased  $T_{MI}$  is limited only to the structural stability.

## References

- [1] M. Kar and S.Ravi, "Metal-Insulator in electron doped Ba<sub>1-x</sub>La<sub>x</sub>MnO<sub>3</sub> Compounds" *Pramana*, 58 [5&6]1009-1012(2002).
- [2] C. Zener "Interaction between the D-Shell in the transition Metals" *Phys. Rev.* 81[5] 440-444(1951). "Ferromagnetic Compounds of Manganese with Perovskite structure" *Phys. Rev.* 82[3] 403-405(1951).
- [3] E. Bose, S.Karmakar and B.K.Chanudhri, "Small polaron hopping conduction and magnetic frustration in the electron-doped charge ordered Ca<sub>0.85</sub>La<sub>0.15</sub>MnO<sub>3</sub> System" *J.Phys.Conds.Matter* 19 486201(8pp) (2007).
- [4] Q. Zhou and B. J. Kennedy, "The nature of the orthorhombic to tetragonal phase transition in Sr<sub>1-x</sub>Ca<sub>x</sub>MnO<sub>3</sub>" *J. Solid State Chem.* 179 3568–3574 (2006).
- [5] B.J.Kennedy, P.J. Saines, Q. Zhou, Z. Zhang, M. Matsuda, M. Miyake. "Structural and electronic phase transitions in Sr<sub>1-x</sub>Ce<sub>x</sub>MnO<sub>3</sub> perovskites" *J.Solid State Chem.* 181 2639–2645 (2008).
- [6] M. Ohtaki, H. Koga, T. Tokunaga, K. Eguchi and H. Arai. "Electrical Transport Properties and High – Temperature Thermoelectric Performance of (Ca<sub>0.9</sub>M<sub>0.1</sub>)MnO<sub>3</sub> (M = Y, La, Ce, Sm, In, Sn, Sb, Pb, Bi)" *J.Solid State Chem.* 120 105-111(1995).
- [7] P. Duan, G. Tan, S. Dai, Y. Zhou, Z. Chen, "Colossal magnetoresistance effect of the electron-doped manganese oxide La<sub>1-x</sub>Sb<sub>x</sub>MnO<sub>3</sub> (x=0.05,0.1)" *J.Phys.: Condens. Matter* 15 4469–4476(2003)
- [8] C.G.Hu, H.Liu, C.S.Cao, L.Y.Zhang, D. Davidovic and Z.L.Wang. "Size-Manipulable Synthesis of Single – Crystalline BaMnO<sub>3</sub> and BaTi<sub>2</sub>Mn<sub>1/2</sub>O<sub>3</sub>" *J.Phys.Chem. B.Lett.* 110 [29] 14050-14054 (2006).
- [9] D. Kim, J. Yoo, I. Kim, and J. Song, "Dielectric and piezoelectric of Bi<sub>2</sub>O<sub>3</sub> added (Pb,Ca,Sr) X(Ti,Mn,Sb))<sub>3</sub> ceramics sintered at low temperature", *J.Appl.Phys* 105 061642(4pp) (2009).
- [10] Y. Akishige, K. Honda and S. Tsukada, "Synthesis and dielectric Properties of Mn-Doped BaTi<sub>2</sub>O<sub>5</sub>" ceramics, *Jap. J. Appl. Phys* 50 09NC10(2011).
- [11] H. Liu, C. Hu and Z. L. Wang, "Composite-Hydroxide – Mediated approach for the synthesis of nanostructures of complex functional –oxides", *Nanoletters*, 6 [7] 1535-1540 (2006).
- [12] W. Liu, Xinfeng, and J. Sharp, "Low – temperature solid state reaction synthesis and thermoelectric properties of high –performance and low-cost Sb-doped Mg<sub>2</sub>Si<sub>0.6</sub>Sn<sub>0.4</sub>" *J.Phys. D: Appl.Phys.* 43 085406(6pp)(2010).
- [13] M.E. Melo Jorge, M.R.Nunes, R.Silva Maria, and D.Sousa "Metal –Insulator Transition Induced by Ce Doping in CaMnO<sub>3</sub>" *Chem. Mater.* 17 [8] 2069-2075 (2005)
- [14] S L Yuan, J. Tang, Z C Xia, L F Zhao, I Liu, W Chen, G H Zhang, L J Zhang, W Feng, Q H Zhong and S Liu, "Effect of sintering temperature on electronic transport and low – field colossal magnetoresistance in sol-gel prepared polycrystals of nominal La<sub>2/3</sub>Ca<sub>1/3</sub>Mn<sub>0.96</sub>Cu<sub>0.04</sub>O<sub>3</sub>" *J. Phys.* 36 1446–1450 (2003).
- [15] Y. H. Kim, D. Kim, C. Sub Lee, "Synthesis and characterization of CoFe<sub>2</sub>O<sub>4</sub> magnetic nanoparticles prepared by temperature –controlled coprecipitation method" *Physica B* 337 42-51 (2003).
- [16] V.A.Blogojevic, J.P.Carlo, L.E.Brus, M.L.Steigerwald, Y.J.Uemura, S.J.L.Billinge, W.Zhou, P.W.Stephens, A.A. Aczel and G.M. Luke, "Magnetic phase transition in V<sub>2</sub>O<sub>3</sub>" *Phy.Rev.B* 82 094453(6pp)( 2010).
- [17] K.Vijayanandhi, T.R.N.Kutty, "Phase Conversions in Calcium Manganites with changing Ca/Mn ratios and their influence on the electrical transport properties", *J.MaterSci: Mater Electron* 20 445-454(2009).
- [18] K.R.Poeppelmeier, M.E.Leonowicz, J.M.Longo, CaMn<sub>0.25</sub> and Ca<sub>2</sub>MnO<sub>3.5</sub>: "New oxygen –defect perovskite –type oxides" *J.Solid State Chem* 44[1] 89-98(1982).
- [19] John Philip and T R N Kutty "Effect of valence fluctuations in A sites on the transport properties of La<sub>1-x</sub>R<sub>x</sub>MnO<sub>3</sub> (R = Ce, Pr)" *J. Phys.: Condens. Matter* 11 8537-8542 (1999)
- [20] F.S. Razavi, G.V.Sudhakar Rao and H.Jalili, H.U.Habermeyer, "Pressure Induced phase transition in periodic micro twinned thin film of La<sub>0.88</sub>Sr<sub>0.1</sub>MnO<sub>3</sub>", *Appl. Phys. Lett* 88, 174103-3(2006).
- [21] J.Klein, J.B.Philipp, G.Carbonwe, A.Vigliante, L.Alff, and R.Gross, "Transport anisotropy in biaxially strained La<sub>2/3</sub>Ca<sub>1/3</sub>MnO<sub>3</sub> thin films", *Phy.Rev.B* 66 052414-4(2002).
- [22] Y. Liu, Y. Li, H. Zhang, D. Chen and Q. Wen, "Study on magnetic properties of low temperature sintering M-Barium hexaferrites", *J.Appl.Phys* 107 09A507-3(2010).
- [23] M. Ziese, "Spontaneous resistivity anisotropy and band structure of La<sub>0.7</sub>Ca<sub>0.3</sub>MnO<sub>3</sub> and Fe<sub>3</sub>O<sub>4</sub> films" *Phys. Rev. B* 62 [2]1044-1050(2000).
- [24] P.Schiffer, A.P.Ramirez, W.Bao and S.W.Cheong, "Low Temperature Magnetoresistance and the magnetic phase diagram of La<sub>1-x</sub>CaxMnO<sub>3</sub>" *Phy. Rev. Lett.* 75 [18]3336-3339(1995).
- [25] X.Wang and X.G.Zhang, "Low–Temperature resistivity in a nearly half-metallic Ferromagnet" *Phys.Rev.Lett* 82[21] 4276-4279(1999).
- [26] Y. Sun, M.B.Salamon, W. Tong and Y. Zhang, "Magnetism, electronic transport, and colossal magnetoresistance of (La<sub>0.7-x</sub>Gdx) Sr<sub>0.3</sub>MnO<sub>3</sub> (0≤x≤0.6)" *Phys. Rev. B* 66 094414-6(2002).
- [27] J.A.Souza and R.F.Jardim, "Magnetoresistivity in the clustered state of La<sub>0.7-x</sub>Y<sub>x</sub>Ca<sub>0.3</sub>MnO<sub>3</sub> manganites" *Phys. Rev. B* 71 0554404(2005).
- [28] P. Sumana Prabhu, M.S. Ramachandra Rao and U.V. Varadaraju, "Tc Suppression and conduction mechanisms in Bi<sub>2-x</sub>Sr<sub>1.93</sub>Ca<sub>0.97-x</sub>R<sub>x</sub>Cu<sub>2</sub>O<sub>8+y</sub> (R=Pr, Gd, and Er) systems" *Phys. Rev. B* 50[10] 6929-6938(1994).

- [29] W. Khan, A. H.Naqvi, M. Gupta, S. Husain and R kumar "Small polaron hopping conduction mechanism in Fe doped  $\text{LaMnO}_3$ " J.Chem. Phys. 135 054501(2011).
- [30] V.Ponnambalam, U.Varadaraju, "Observation of variable-range hopping up to 900K in the  $\text{YLa}_x\text{Ba}_{2-x}\text{Cu}_3\text{O}_{7-\delta}$  system", Phys. Rev. B 52[22] 16213-16216(1995).
- [31] Hwang H Y, Cheong S W, Ong N P and Batlogg B, " Spin polarized intrgrain tunneling in  $\text{La}_{2/3}\text{Sr}_{1/3}\text{MnO}_3$ ",Phys. Rev. Lett. 77[10] 2041-2044(1996).
- [32] Chang-Yi Chou,N.Kavrav, Yung-Kang Kuo and Dong – HaiKuo, "Electrical properties of A/B-site substituted Ni-deficient  $\text{La}(\text{Ni}_{0.6}\text{Fe}_{0.3})\text{O}_3$  Perovskites with  $\text{A} = \text{Ag}^+, \text{Pd}^{2+}, \text{Nd}^{3+}$  and  $\text{B} = \text{Mn}^{3+}, \text{Ga}^{3+}$ " J.Appl.Phys. 103 093716-7(2008).
- [33] O. Chmaissem, B.Dabrowski, S.Kolesnik, J.Mais, D.E.Brown, R.Kruk, P.Prior, B.Pyles, and J. D. Jorgensen, "Relationship between structural parameters and the Neel temperature in  $\text{Sr}_{1-x}\text{Ca}_x\text{MnO}_3 (0 \leq x \leq 1)$  and  $\text{Sr}_{1-y}\text{Ba}_y\text{MnO}_3 (Y \leq 0.2)$ " Phys. Rev B. 64 134412-9(2001).
- [34] Lide M. Rodriguez-Martinez and J. Paul Attfield, "Cation disorder and size effects in magnetoresistive manganese oxide perovskites" Phys. Rev. B 54 R15 622(1996).
- [35] K.Padmavathi, G.Venkataiah, P.Venugopal Reddy," Electrical behavior of some rare-earth –doped  $\text{Nd}_{0.33}\text{Ln}_{0.34}\text{Sr}_{0.33}\text{MnO}_3$  manganites" J. Magn. Mater. 309 237-243(2007).
- [36] S. Bhattacharya, S. Pai, R.K.Mukherjee, B.K.Chaudhuri, S.Neeleshwar, Y.Y.Chen, S.Mollah and H.D.Yang, Development of pulsed magnetic field and study of magnetotransport properties of K-doped  $\text{La}_{1-x}\text{Ca}_x\text{K}_y\text{MnO}_3$  CMR materials J. Magn. Mater. 269 359-371(2004).
- [37] E.K Abdel-Khalek, W.M. EL-Meligy, E.A. Mohammed, T.Z. Amer and H.A. Sallam."Study of relationship between electrical and magnetic properties and Jahn- Teller distortion in  $\text{R}_{0.7}\text{Ca}_{0.3}\text{Mn}_{0.95}\text{Fe}_{0.05}\text{O}_3$ " J. Phys. Condens. Matter 21 026003(2009).
- [38] J.C.Grenier, M.Pouchard, P.Hagenmuller, "Vacancy ordering in oxygen –deficient Perovskite –related ferrites" Structu.Bond. 47 1(1981).
- [39] W. Hwan Jung, "Variable range hopping conduction in  $\text{Gd}_{1/3}\text{Sr}_{2/3}\text{FeO}_3$ " Physica B 304 75-78(2001).
- [40] Y. Wang, Y. Sui, J. Cheng, X. Wang, Z. Lu, and W. Su, "High Temperature Metal – Insulator Transition Induced by Rare-Earth doping in perovskite  $\text{CaMnO}_3$ " J.Phys.Chem.C. 13 12509-12516(2009)